Grain Boundary Segregation of an Al-Zn-Mg Ternary Alloy

J. M. CHEN, T. S. SUN, R. K. VISWANADHAM, AND J. A. S. GREEN

Auger electron spectroscopy (AES) has been used to measure the grain boundary concentration profiles of alloy additions in an Al-5.5 pct Zn-2.5 pct Mg ternary in as-quenched, under-, peak-, and over-aged conditions. The AES depth profiles show marked segregation of Mg and Zn to the grain boundary, in contrast to that reported previously on similar Al alloys. It is found that this apparent contradiction can be resolved by exploiting the plasmon-loss features of the AES spectra to help elucidate the grain boundary segregation. With the AES/plasmon-loss measurements, one can determine not only the concentration of Mg and Zn at the grain boundary, but also the metallurgical environments surrounding the alloy additions. It is shown that, for over-aged specimens of the Al alloy, only a fraction of the total Mg at the grain boundary is incorporated in $MgZn_2$ precipitates, the remainder being segregated to within a few atomic layers of the boundary.

GRAIN boundary segregation of alloy components and impurities has been known for some time.[1] The relation between this phenomenon and the mechanical properties of metals could not be quantitatively studied, however, until the advent of Auger electron spectroscopy (AES).[2-4] The shallow probing depth (10-20 A) of AES revealed that the segregated elements can be localized to the top few atomic layers of the grain boundary. Thus, AES has been extremely useful in determining the chemical composition of grain boundary surfaces which can then be correlated with other metallurgical properties of materials.

In the case of Al-Zn-Mg alloys, AES studies[5] have shown that the alloying elements Mg and Zn are heavily segregated to the grain boundaries. Transmission electron microscopy (TEP) studies[6,7] have shown that for aged Al-Zn-Mg alloys, the segregated elements form $MgZn_2$ precipitates, and as a consequence, there exists a precipitate free zone (PFZ) at both sides of the grain boundary. The composition and mechanical properties of the PFZ has been the focus of several studies on the stress corrosion of aluminum alloys since cracking in these alloys is intergranular. Recent mechanistic studies[8-10] have indicated that crack propagation may occur due to hydrogen embrittlement, as opposed to anodic dissolution[11] as previously suggested. In conducting additional measurements of the alloy composition immediately adjacent to the grain boundary to further investigate the mechanism of cracking, it became clear that there are considerable contradictions in the literature with regard to grain boundary segregation in these alloys.

For example, Doig and Edington[12-14] reported measurements of Mg content near the grain boundaries of Al-5.9 pct Zn-3.2 pct Mg alloys in as-quenched, under-, peak-, and over-aged conditions. By monitoring the plasmon loss of the electron beam in a TEM, Doig and Edington were able to determine the *spatial distribution* of Mg as the electron beam was traversed across a grain boundary. The situation is depicted by the trace a-a' in Fig. 1(a). For as-quenched specimens, Doig and Edington found an accumulation of Mg at the grain boundary. On the other hand, for over-aged specimens, their measurements showed a *depletion* of Mg in the PFZ, the Mg content decreasing from the bulk value of 3.2 pct to about 0.2 pct at the boundary. Some of Doig and Edington's data[14] are reproduced in Fig. 1(b) and (c). The above results were interpreted with the model that, in the over-aged case, a major portion of Mg at the grain boundary combine to form the $MgZn_2$ precipitates, leaving the region between the precipitates depleted in Mg.

Recently, Green *et al*[15] also have measured the grain boundary composition of Ag-Zn alloys of similar composition in the as-quenched, peak and over-aged conditions. AES and argon ion sputtering were used to obtain the chemical depth profiles of grain boundary surfaces. The AES measurements showed, however, an *accumulation* of Mg at the grain boundary under all conditions.

In this paper, we demonstrate that the apparent contradiction between the T. M/plasmon loss results of Doig and Edington and the AES results of Green *et al*, can be resolved by exploiting the plasmon loss features of the AES spectra to help elucidate the segregation/precipitation problem. Specifically, it is found that the plasmon loss energy measurements in the TEM and the AES techniques provide different, but complementary, information about the grain boundary. A combination of these two techniques has led to a better understanding of segregation effects at grain boundaries.

EXPERIMENTAL METHODS AND MATERIALS

The Auger electron spectrometer used in this study is a Physical Electronics, double-pass cylindrical mirror analyzer (system model 548). The spectrometer includes an ultra high vacuum system (UHV), where the experiments were conducted under a basal

J. M. CHEN is Head, T. S. SUN is Research Scientist, Physics Department, R. K. VISWANADHAM is Research Scientist, Material Science Department, and J. A. S. GREEN is Associate Director, Martin Marietta Laboratories, Baltimore, MD 21227.

Manuscript submitted April 15, 1977.

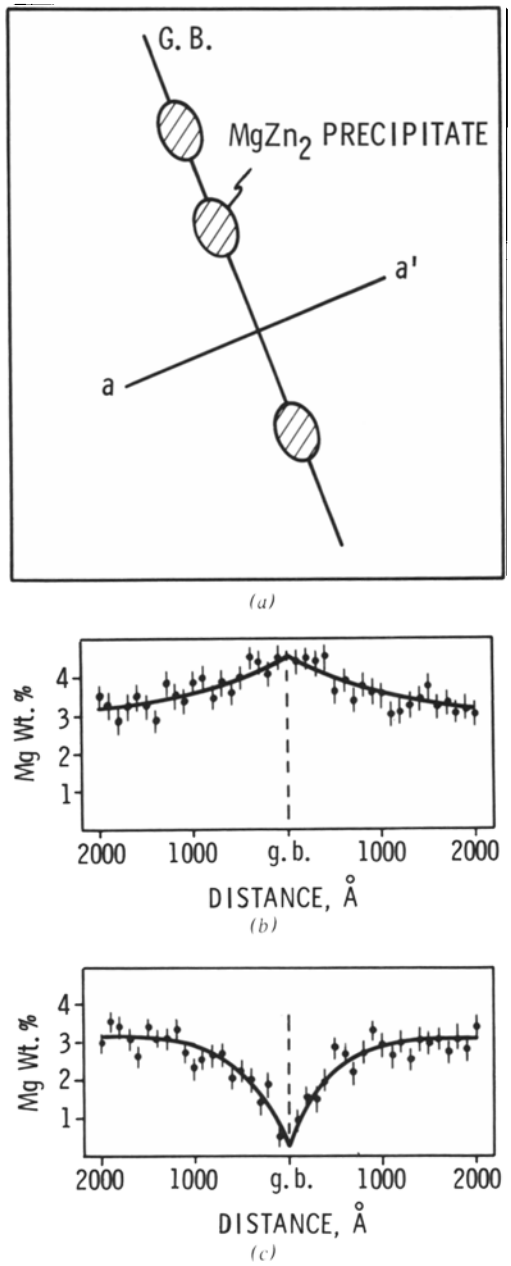

Fig. 1–(*a*) Schematic diagram of $MgZn_2$ precipitates at a grain boundary, a-a' represents the line along which microanalysis of Mg concentration is performed by the TEM/plasmon loss technique. (*b*) Water quenched from 500°C and (*c*) air cooled from 500°C are Mg concentration profiles across grain boundaries in Al-5.9 pct Zn-3.2 pct Mg alloys as measured by Doig and Edington (Ref 14)

pressure $<5 \times 10^{-10}$ torr. Ar ion sputtering was employed to mill the specimen in order to obtain Auger depth profiles. A fracture device, utilizing a shear-to-break configuration, was used for *in situ* fracture experiments. To obtain quantitative data, the Auger peak-to-peak height of each element was measured, and weighed with an appropriate sensitivity factor to evaluate its atomic percentage.[16]

The high purity ternary used for these investigations had a composition of 5.49 wt pct Zn and 2.47 wt pct Mg (total impurity <0.1 wt pct, individual impurity <0.01 wt pct). Strips 1 mm thick were solution treated in dry argon at a temperature of 475°C for 10 min and water quenched. The grain size for the solution treated specimens was about 0.08 mm. The quenched samples were then heat treated at 130 and 160°C for 4.5, and 22 h to obtain the under, peak, and over-aged conditions. Small strips were then cut from the samples, notched, and transferred to the spectrometer.

RESULTS

A) Auger Depth Profiles

A scanning electron micrograph of the fractured surface of an aged sample is shown in Fig. 2. The as-quenched samples show a combination of inter- and transgranular fractures. On the other hand, the peak and over-aged samples show definite intergranular fracture. In this paper, we are concerned mainly with the fractured surfaces of aged samples. It is clear from Fig. 2 that AES measurements on these samples will be probing predominantly the grain boundary surfaces.

A typical Auger spectrum taken from the fractured surface of an over-aged sample (160°C for 22 h) is shown in Fig. 3. The grain boundary depth profiles for Mg and Zn, obtained on the ternary alloy in different heat treated conditions, are shown in Figs. 4 and 5 respectively. The age-hardening curves at these two temperatures are superimposed on the profiles. We note several important features in these figures:

(i) The Auger spectrum for the over-aged grain boundary surface (Fig. 3) indicates the presence of the

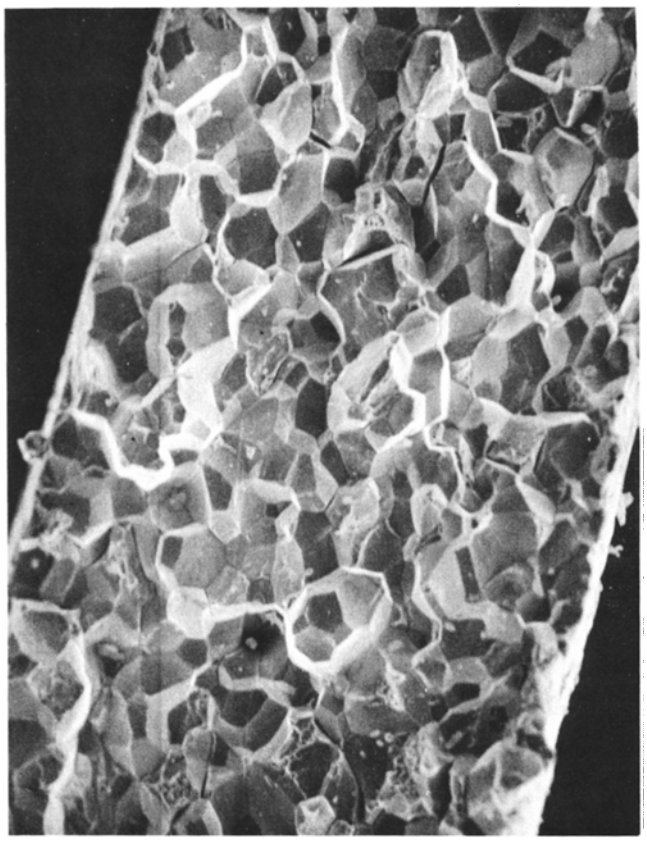

Fig. 2–Scanning electron micrograph of the fracture surface of a quenched and aged high purity Al-Zn-Mg ternary alloy. The grain size is approximately 0.08 mm (magnified 97 times).

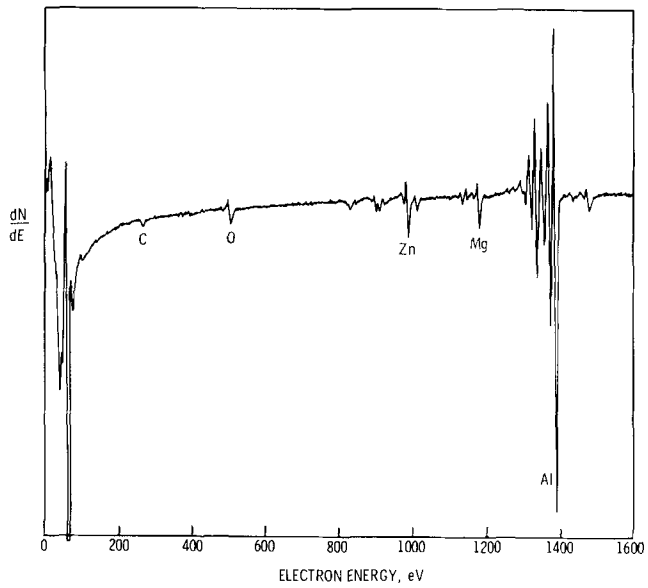

Fig 3–Auger electron spectrum from the fracture surface of an overaged high purity ternary alloy.

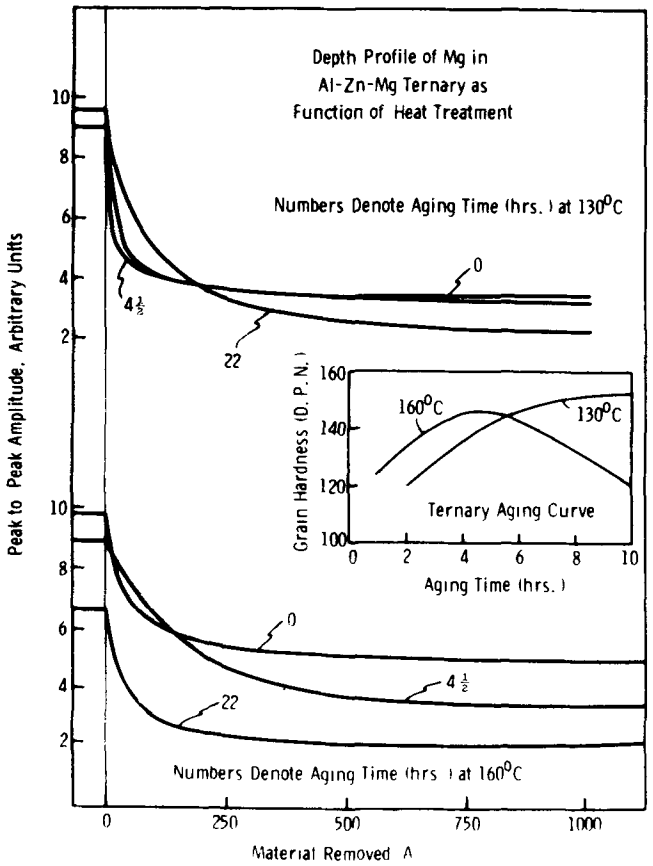

Fig. 4–Chemical depth profiles for Mg in Al-Zn-Mg ternary alloys as a function of heat treatment. The aging curves at 130 and 160°C are shown in the insert. (D. P. N. is given in Kg/mm^2.)

alloy additions Mg and Zn. The Auger peak-to-peak amplitudes can be converted to atomic percentages.[16] Such conversions give ~5.4 at. pct for Mg and ~4.5 at. pct for Zn. If all the Mg and Zn segregation were exclusively due to $MgZn_2$ precipitates the Mg to Zn ratio should be 1:2. Therefore, it is clear, as already pointed out by Green *et al*,[15] that in addition to $MgZn_2$ precipitates, the grain boundary contains excess Mg.

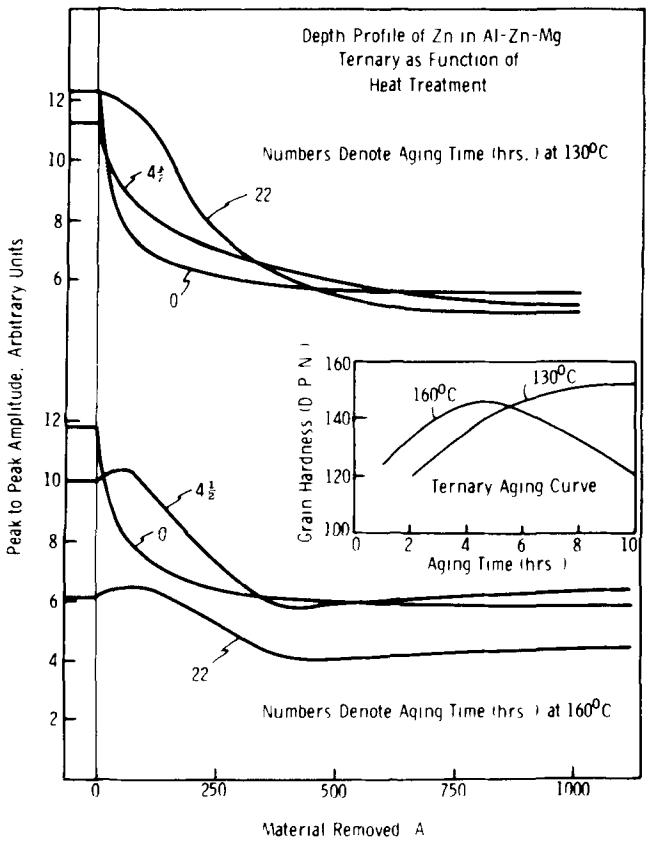

Fig. 5–Chemical depth profiles for Zn in Al-Zn-Mg alloys as a function of heat treatment. The aging curves are shown in the insert (D. P. N. is given in Kg/mm^2.)

(ii) The above observations can be substantiated further by comparing Fig. 3 with the Auger spectrum of a $MgZn_2$ alloy* which is shown in Fig. 6. Such a direct comparison of Auger amplitudes eliminates any uncertainty involved in estimating Auger sensitivities for Mg and Zn. The Zn/Mg Auger peak height ratio in Fig. 3. is about 1:0.75 while for the $MgZn_2$ alloy is about 1:0.28. Thus, if we assume that all the Zn atoms on the grain boundary surface of the over-aged sample were incorporated in the second phase particles, then 40 pct of the total grain-boundary Mg would be accounted for in the $MgZn_2$ precipitates themselves and the remaining 60 pct would be outside the precipitates.

*The authors are grateful to Dr. F. Cocks for preparing the sample of $MgZn_2$ intermetallic.

(iii) As shown in Fig. 4, under *all* heat treatment conditions, there is a marked segregation of Mg to the grain boundaries. The grain boundary concentrations are several times the bulk concentration. This is in sharp contrast to the results of Doig and Edington as sketched in Fig. 1(*b*) and (*c*). They observed a much less dramatic accumulation of Mg at the grain boundary for as-quenched samples and a depletion of Mg for over-aged samples.

(iv) The width of the segregation zone, which can be defined by the point where the Mg concentration decreases to the arithmatic mean between the grain boundary and bulk concentrations, varies from about 10Å for the as-quenched samples to about 100Å for the over-aged samples, see Fig. 4. These results are also in contrast to the Doig and Edington data of the

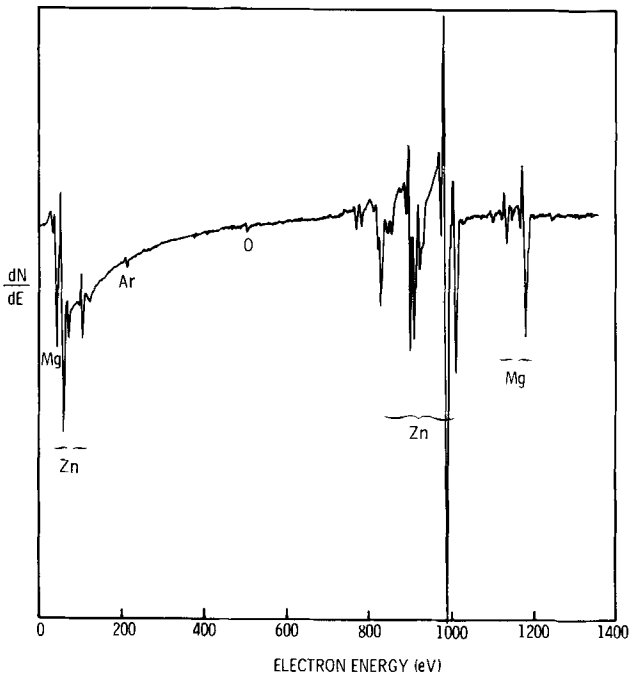

Fig. 6–Auger electron spectrum of a $MgZn_2$ alloy surface.

as-quenched specimen, where the width, as measured by the TEM/plasmon loss technique, is about 500Å.

(v) Since the plasmon energy of Al alloys depends only weakly on the concentration of Zn addition,[17] the TEM/plasmon loss measurement cannot provide the concentration profile for Zn. As shown in Fig. 5, AES measurements indicate a similar grain boundary segregation of Zn. In the over-aged cases, however, the depth profile for Zn is distinctively different. Instead of a very rapid initial decrease, it shows a plateau at the grain boundary. As a consequence, the segregation is extended to about 200Å.

B) Plasmon Loss of Auger Electrons

In AES measurements on metallic surfaces, one measures not only the Auger electrons ejected into the vacuum without energy loss, but also the Auger electrons that have suffered plasmon losses. The latter give rise to a satellite peak on the low energy side of the Auger peak. Its energy position relative to the Auger peak is determined by the plasmon energy and can be measured accurately. Since the plasmon energy is a function of the electron density of the medium that the escaping Auger electrons penetrate, the Auger electron-induced plasmon loss satellites can provide information about the environment surrounding the particular chemical species of interest. In particular, the plasmon energy losses measured in Al and in $MgZn_2$ alloy are 15.8 ± 0.2 and 12.0 ± 0.2 eV respectively. Thus, an energy loss of 15.8 eV should be observed for the Mg atoms in solution near the grain boundary and an energy loss of 12.0 eV for the Mg atoms in the $MgZn_2$ precipitates.

Fig. 7 shows portions of high resolution Auger spectra of Al-Zn-Mg alloys. Our focus is on the 994 eV (Zn), 1186 eV (Mg) and 1396 eV (Al) Auger peaks. As indicated, there is a plasmon-loss satellite associated with each Auger peak, and the plasmon energy losses are different for as-quenched and

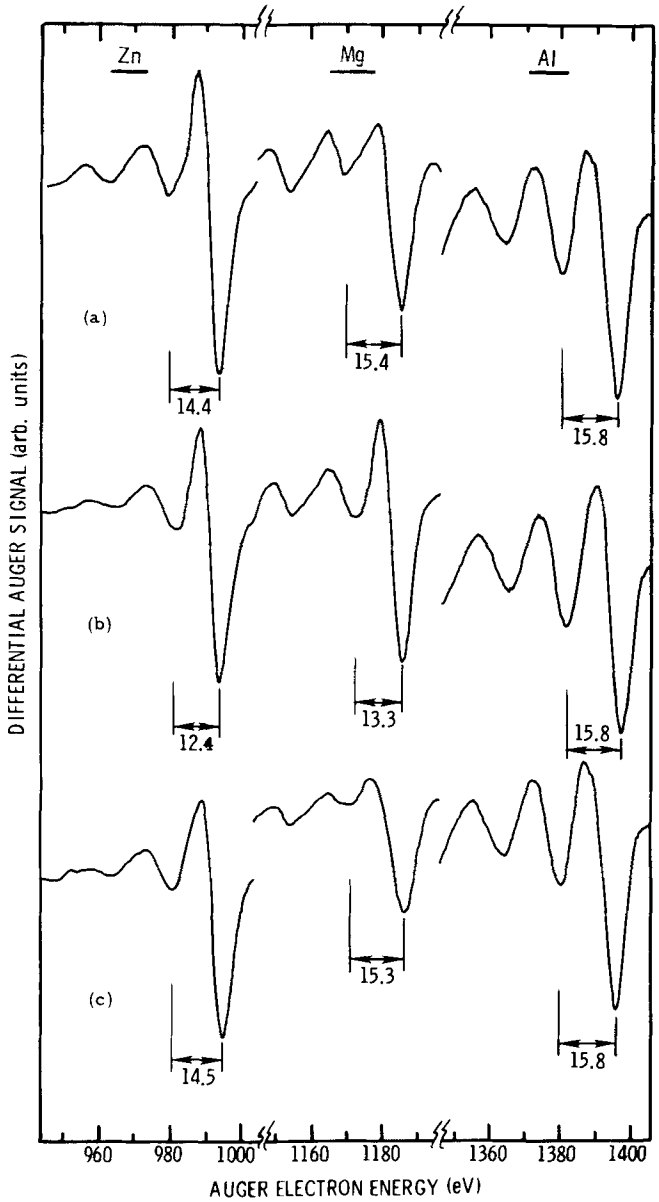

Fig. 7–Auger electron spectra for the elements Zn, Mg and Al of the Al-Zn-Mg alloy in as-quenched (row (*a*)) and over-aged (row (*b*)) conditions. The spectra representing the bulk of the alloy is shown in row (*c*).

over-aged conditions. The Auger spectrum for the sputtered condition was obtained after sufficient material on the grain boundary was removed by Ar ion bombardment until the bulk composition of the alloy was reached.

The plasmon energy losses for the Al-Zn-Mg alloys, together with that for $MgZn_2$, are summarized in Table I. We note several interesting points:

(i) The plasmon loss energy for the Al Auger peak is constant at 15.8 ± 0.2 eV for as-quenched, over-aged and sputtered samples. This is understandable because the alloy additions constitute only a few percent of the Al alloy, so the majority of Al Auger electrons escape through a medium of essentially pure Al metal.

(ii) For the over-aged samples, the plasmon loss energy for the Mg Auger peak is 13.3 ± 0.2 eV, appreciably *higher* than that in $MgZn_2$ (12.0 ± 0.2 eV), and increases to 15.3 ± 0.2 eV when the bulk of the

Table I. Measured Plasmon Loss Energies in $MgZn_2$ and Al-Zn-Mg Alloys

	Zn	Mg	Al
$MgZn_2$	12.0 ± 0.2 eV	12.0 ± 0.2	–
Al-Zn-Mg as quenched	14.4 ± 0.2	15.4 ± 0.2	15.8 ± 0.2
Al-Zn-Mg over aged	12.4 ± 0.2	13.3 ± 0.2	15.7 ± 0.2
Al-Zn-Mg sputtered	14.5 ± 0.2	15.3 ± 0.2	15.8 ± 0.2

grain is reached after sputtering. We believe this result is significant. It provides additional support to the picture that only a fraction of the total Mg at the grain boundary is associated with $MgZn_2$, the rest is at the grain boundary situated outside of the precipitates.

(iii) The plasmon losses for the as-quenched samples do not change on sputtering. Thus, although there is an appreciable segregation of both Mg and Zn to the grain boundary for the as-quenched samples, the *chemical states* of Mg and Zn appear to be the *same* at the grain boundary as in the bulk.

(iv) For the over-aged samples, the plasmon loss energy for the Zn Auger peak is 12.4 ± 0.2 eV, nearly the same as that measured in $MgZn_2$. This result suggests that, for the over-aged samples, *all* the Zn atoms at the grain boundary are in the $MgZn_2$ precipitates.

The plasmon loss in the as-quenched samples (14.4 ± 0.2 eV for Zn and 15.4 ± 0.2 eV for Mg), are consistently lower than that for Al (15.8 ± 0.2 eV). This suggests that even for as-quenched samples there is some degree of precipitate formation (probably Guinier-Preston zones) throughout the bulk of the material.

DISCUSSION

The above AES plasmon loss results indicate that, at the grain boundary of over-aged samples, the Zn atoms are all in the form of $MgZn_2$ precipitates. On the other hand, only about 40 pct of total Mg is in the precipitates, the other 60 pct of Mg being localized to within a few atomic layers of the grain boundary. In this section, we will utilize these findings in an attempt to resolve the apparent contradiction between the TEM/plasmon-loss and the AES/plasmon loss data.

An important factor that must be taken into consideration when comparing the AES and TEM data is the vast difference in spatial resolution of these two techniques. In TEM, the electron beam is typically less than 100Å (10^{-2} μm) in diameter while the electron beam used in our Auger measurement was about 200 μm in diameter. Therefore, the Auger data represent a measure of Mg content averaged over an area of 200 μm in diameter on the fracture surface, which corresponds to about 10 grains for the grain size employed (~0.08 mm). On the other hand, the TEM Mg profile was obtained by traversing the 100Å electron beam across the grain boundary *in between* the $MgZn_2$ precipitates[12] as depicted in Fig. 1(*a*). Therefore, when interpretating the AES data, the contribution from the $MgZn_2$ precipitates should certainly be included.

Also, due to experimental limitations, the TEM technique is not capable of measuring Mg content to within 50Å of the grain boundary. Therefore, any accumulation of Mg localized to within a few atomic layers of the grain boundary will *not* be detected by the TEM/plasmon loss measurement. On the other hand, the AES technique, being a surface sensitive tool, is ideally suited to detect just such accumulations.

The TEM/plasmon-loss technique measures the Mg concentration *within* the grains, but not the Mg concentration *at* the grain boundary, while the AES depth profile includes contributions from both. Therefore, to interpret the AES Mg depth profile data, we should add to the concentration profile of Doig and Edington the contributions from the precipitates as well as the Mg localized at grain boundary. Since we have deduced from the plasmon-loss satellite measurement that for the over-aged samples, *all* of Zn at the grain boundary is incorporated in the precipitates, we conclude from the Auger peak-to-peak amplitude information of Figs. 3 and 6 that about 40 pct of Mg is associated with $MgZn_2$ and the remainder is outside the precipitates.

A schematic illustration of the various contributions to the Mg depth profile of the over-aged samples is shown in Fig. 8(*a*). The total Mg profile (Curve *a*) is the sum of the profile at the grain boundary (Curve *b*), the profile within the grain (Curve *c*) and the profile of the precipitate (Curve *d*). As outlined in the following paragraphs, the width

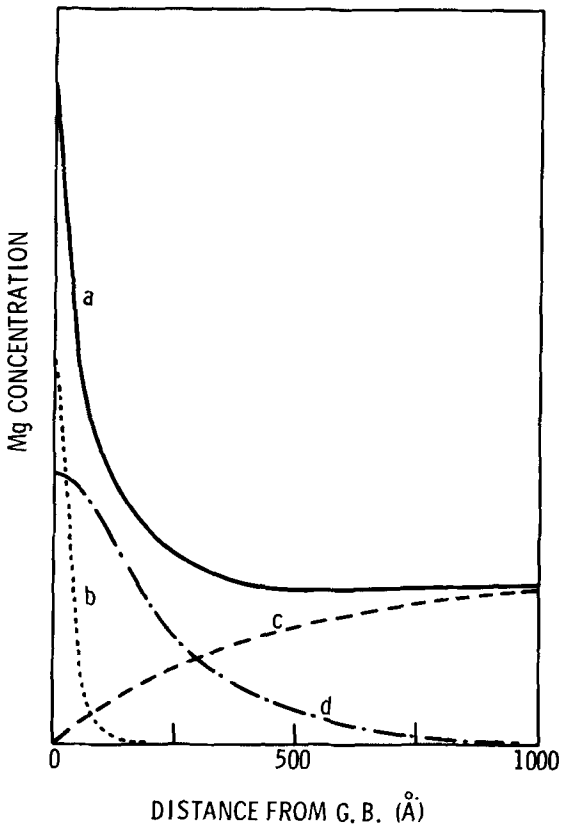

Fig. 8(*a*)–Schematic diagram of various contributions to the Mg depth profile for overaged samples. (a, resultant profile; b, profile at G.B.; c, profile in PFZ; d, profile of precipitates).

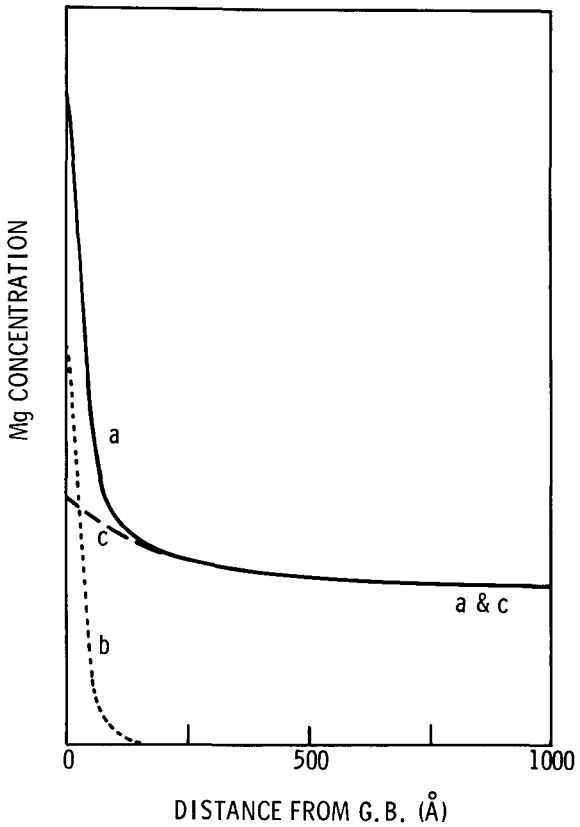

Fig. 8(*b*)—Schematic diagrams of various contributions to the Mg depth profile for as-quenched samples. (a, resultant profile; b, profile at G.B.; c, profile in PFZ.)

of Curve *d* is estimated from the measured concentration profile for Zn. As seen, the total Mg profile resembles closely those shown in Fig. 4.

Similarly, we can construct a Mg depth profile for the as-quenched samples. Because of the absence of grain boundary precipitates in this case, the profile can be obtained by simply adding to the profile within the grain of Doig and Adington (Curve *c*) a narrow profile representing the grain boundary Mg contribution (Curve *b*). This is shown in Fig. 8(*b*). Note that due to the absence of precipitates, the total Mg profile in Fig. 8(*b*) is steeper than that of Fig. 8(*a*), consistent with the AES data on Fig. 4. Thus, by taking into account the various contributions to the Mg depth profile, the apparent contradiction between the TEM/plasmon-loss and AES measurement can be resolved.

As pointed out in Section A, for the over-aged samples, the depth profiles for Zn show a plateau at the grain boundary. In light of the above discussion, this is now easily understandable: in the over-aged cases, all the Zn atoms are incorporated in the $MgZn_2$ precipitates. The AES depth profile simply maps out the concentration profile of the precipitates. The as-quenched samples as well as the 130°C, 4.5 h aged sample do not have grain boundary precipitates (Fig. 5). On the other hand, the samples aged at 130°C for 22 h, 160°C for 4.5 h and 22 h show clear evidence of precipitate formation. The size of the precipitates, as shown in Fig. 5, is about 200Å. This information was used to estimate the width of the precipitate-contribution to the total Mg profile (Fig. 8(*a*)).

SUMMARY AND CONCLUSIONS

AES measurements have been used to determine the concentration profiles of Mg and Zn at grain boundaries of an Al-Zn-Mg ternary under different aging conditions. The AES depth profiles show sharp segregation of Mg and Zn to the grain boundary, more marked than those reported by Doig and Edington on similar Al alloys. In the case of samples containing precipitates, the AES results were in apparent contradiction to those reported by Doig and Edington using TEM/plasmon-loss measurements.

We have shown that plasmon energy losses in the Auger spectrum can be exploited to help elucidate the precipitation/segregation picture. With the measured Auger amplitude and plasmon-loss information, we are able to determine not only the concentration of Mg and Zn at the grain boundary but also the chemical environments of the alloying additions.

It is found that, for both the as-quenched and over-aged samples, there is a marked segregation of Mg and Zn to the grain boundary; and that for the over-aged samples about 40 pct of the total Mg at the grain boundary is incorporated in $MgZn_2$ precipitates while the remaining Mg is segregated to within a few atomic layers of the grain boundary.

Based on the above information, together with the recognition that TEM/plasmon-loss and AES techniques measure different aspects of the grain boundary, it is possible to resolve the apparent contradictions between the results of these two techniques. These two techniques provide different, but complementary information, about the grain boundary. A combination of these techniques has led to an improved picture of grain boundary segregation in Al-Zn-Mg alloys.

ACKNOWLEDGMENTS

The authors acknowledge financial support of the Office of Naval Research (Contract No. N00014-74-C-0277) and are grateful to P A. Clarkin for his constant encouragement.

REFERENCES

1 J. H. Westbrook: *Metals Rev.*, 1964, vol. 9, p. 415.
2. H. L. Marcus and P. W. Palmberg. *Trans TMS-AIME*, 1969, vol. 245, p. 1664
3 D. F. Stein, A. Joshi, and R P. LaForce: *Trans. ASM*, 1969, vol. 62, p. 776.
4 H Ohtani, H C Feng, and C. J. McMahon, Jr.: *Met. Trans.*, 1974, vol. 5, p. 516
5. J. A. S. Green and W. G. Montague: *Corrosion*, 1975, vol 31, p. 209.
6. A. Kelly and R. B. Nicholson *Prog Mater. Sci.*, 1963, vol. 10, p 151.
7 A. J. Cornish and M. K. B. Day: *J. Inst. Metals*, 1969, vol. 97, p. 44.
8 J. A. S. Green, H. W. Hayden, and W. G. Montague *Effect of Hydrogen on Behavior of Materials*, A. W. Thompson and I. M. Bernskin, eds., p. 200, Publ. Met. Soc. AIME, 1976.
9. G M. Scamans, R. Alani, and P R. Swann: *Corrosion Sci.*, 1976, vol. 16, no. 7, p 443
10 R. J. Gest and A. R. Troiano: *Corrosion*, 1974, vol. 30, p 274.
11 A J. Sedricks, J. A. S Green, and D. L Novak. NACE-3, p. 569, National Association of Corrosion Engineers, Houston, 1974.
12. P. Doig and J. W. Edington: *Brit. Corros. J.*, Quarterly, 1974, vol. 9, p. 220.
13. P. Doig and J. W. Edington: *Brit. Corros. J.*, Quarterly, 1974, vol. 9, p. 461.
14 P. Doig and J. W. Edington. *Met. Trans. A*, 1975, vol. 6A, p. 943.
15. J A. S Green, R. K Viswanadham, T. S. Sun, and W. G. Montague· Martin Marietta Labs., Baltimore, Md., unpublished research, 1977.
16. P. W. Palmberg, G. E. Riach, R. E. Weber, and N. C. MacDonald: *Handbook of Auger Electron Spectroscopy*, p. 14, Physical Electronics Industries, Edina, Minnesota, 1976
17. R. F. Cook and S. L. Cundy: *Phil. Mag.*, 1969, vol. 20, p. 665.